

FERROMAGNETIC RESONANCE IN NANOMETRIC MAGNETIC SYSTEMS

D. S. Schmool^{*}, R. Rocha, J. B. Sousa, J. A. M. Santos, G. N. Kakazei^a, J. S. Garitaonandia^b,
D. Martín Rodríguez^b, L. Lezama^c, J. M. Barandiarán^d

IFIMUP and Departamento de Física, Universidade do Porto, Rua do Campo Alegre 687,
P – 4169 007 Porto, Portugal

^aDepartment of Physics, Ohio State University, Ohio, USA

^bFisika Aplikatua II saila, Euskal Herriko Unibersitatea (UPV/EHU), Apartado 644,
48080 Bilbao, Spain

^cDepartamento de Química Inorgánica, Universidad del País Vasco, Apartado 644, 48080
Bilbao, Spain

^dDepartamento de Electricidad y Electrónica, Universidad del País Vasco, Apartado 644,
48080 Bilbao, Spain

Nanometric magnetic systems are of growing importance, displaying novel magnetic properties which are of both fundamental scientific interest as well as of practical importance. There are several types of system which can be classified as nanometric, which depend on the fabrication process, for example, amorphous / nanocrystalline alloys, immiscible alloys (e. g. Co – Cu), nanostructured films and discontinuous multilayer systems. In whatever case, magnetic confinement effects and the interactions between magnetic particles, via an intervening phase, give rise to the particular magnetic behaviour and properties of the system in question. Ferromagnetic resonance (FMR) is a powerful technique for the study of magnetic properties and has been applied to many different types of magnetic system. FMR essentially measures the internal effective field to which a spin system is subject and as such can reveal useful information on fundamental magnetic properties such as the g – factor, magnetisation, magnetocrystalline anisotropies and shape effects. In the present paper we present experimental results of FMR studies of FeZrCuB amorphous/nanocrystalline alloy, FeAl cluster systems and the discontinuous multilayer system $\text{Al}_2\text{O}_3[\text{CoFe}(t)/\text{Al}_2\text{O}_3]_{10}$, where t is the effective thickness, ranging from 7 to 13 Å.

(Received April 26, 2004; accepted June 3, 2004)

Keywords: Ferromagnetic resonance, Nanostructured magnetic materials, Discontinuous multilayers

1. Introduction

In a magnetic resonance experiment, a spin, whether electronic or nuclear, will precess about the direction of an applied magnetic field when the resonance condition is satisfied by the application of the appropriate strength magnetic (static and rf) field. In the case of nuclear spins this is termed nuclear magnetic resonance (NMR), while in the case of electronic spins the phenomenon is labelled in function of the type of material in question. For example, in paramagnetic materials it is referred to as electron paramagnetic resonance (EPR), also known as electron spin resonance (ESR) and in ferromagnetic materials as ferromagnetic resonance (FMR). There are further classifications, such as antiferromagnetic resonance (AFMR) and spin wave resonance (SWR), which apply to antiferromagnetic and ferromagnetic systems (where confinement effects via magnetic boundaries can permit the excitation of standing spin wave modes of oscillation), respectively.

^{*} Corresponding author: dschmool@fc.up.pt

In the simplest case, electron paramagnetic resonance, the spin system consists of electronic spins which precess around the direction of the applied magnetic field, the angular frequency of which is given by the Larmor equation, $\omega_L = \gamma H$, where γ is the magnetogyric ratio and H the applied field. In the case of ferromagnetic systems, where there is a strong exchange interaction between neighbouring spins, corrections must be introduced due to the internal field created by, for example, exchange field, demagnetising effects and the various magnetic anisotropies which can be present. In a typical EPR/FMR experiment we measure the absorption of microwaves, of fixed frequency, as a function of an externally applied sweep field. The maximum of this absorption is defined as the resonance field. This is essentially a measure of the internal field of a ferromagnetic sample. To assess the contributions to this field we can perform angular studies, varying the direction of the applied field with respect to the sample.

In recent years there has been much research effort directed towards the study of nanostructured magnetic materials. This class of materials generally applies systems where there are two distinct phases, one of which has nanometric dimensions. There are many different preparation techniques which determine the nature of the nanostructure of the samples. While we shall not discuss the various techniques (see refs. [1, 2] for fabrication methods), we can distinguish between the types of nanostructured materials of interest in magnetic studies: samples where there is a definite ordered nanostructuring via precision fabrication (e.g. e-beam lithography) and randomly oriented nanograins in either a ferromagnetic or nonmagnetic matrix. While the former is specifically designed to perform a certain application or study specific aspects of the nanostructure, the latter have a certain intrinsic randomness with regards to size and orientation of the nanostructures, the specifics of which depend on the preparation technique used and any post growth treatments.

Ferromagnetic resonance is a very sensitive magnetic measurement technique which has been applied to virtually all types of known magnetic materials. While FMR can reveal bulk magnetic properties of these materials from the resonance field, it can also provide useful information regarding the microstructure of the samples in question via resonance field and linewidth variations [3]. FMR studies in nanometric systems have been reported for regular ordered nanostructured systems [2] and for certain random grain systems [1]. The latter can be more complex in interpretation due to the random nature of the materials and magnetic interactions between magnetic particles, it is to this latter problem that we are concerned in this paper. In particular we shall discuss some aspects of FMR measurements in materials with randomly oriented nanograins, considering the following systems: $\text{Fe}_{87}\text{Zr}_6\text{B}_6\text{Cu}_1$ melt spun ribbons after various annealing treatments of the amorphous precursor; $\text{Fe}_x\text{Al}_{1-x}$ melt spun ribbons, where x varies from 0.695 to 0.725; the discontinuous multilayer system: $[\text{Al}_2\text{O}_3/\text{CoFe}(t)]_{10}\text{Al}_2\text{O}_3$, where t indicates the equivalent thickness which was varied between 7 and 13 Å.

2. Experimental

The FeZrCuB and FeAl samples were produced using the melt spinning technique in a controlled environment [4, 5]. The annealing treatment of the FeZrCuB samples was performed isochronally at a preset temperature (from 350 – 650 °C) for 1 h under an Ar atmosphere [4, 6]. For the FeAl samples, the samples were subject to the following annealing treatment: 900 °C for 2h and 520 °C for 1 week to produce homogeneous samples which display the bulk like properties as indicated in the FeAl phase diagram [7], the structures were polycrystalline, as verified by x-ray diffraction measurements. The melt spun ribbons were cut into roughly square shapes for measurements. The $[\text{Al}_2\text{O}_3(40\text{Å})/\text{CoFe}(t)]_{10}\text{Al}_2\text{O}_3$ discontinuous multilayers were prepared by Xe ion beam sputtering on to glass substrates, further details of the sample preparation are given in ref. [8, 9]. We note that t is the effective equivalent thickness of $\text{Co}_{80}\text{Fe}_{20}$ without being a continuous film, i.e. form CoFe islands in an Al_2O_3 matrix. Therefore the samples with $t = 7, 9, 11$ and 13 Å represent samples with increasing average island size and density, TEM measurements indicating that the island size is of the order of 1.3 nm [8]. The Al_2O_3 matrix is insulating, so we would only expect magnetic interactions via a dipolar mechanism. Since the distance between the CoFe “layers” is 40

Å, interactions between layers are expected to be almost negligible while those in the plane will be dominant. Therefore we can view the system as virtually a 2D granular material.

The ferromagnetic resonance measurements were performed using a Bruker ESP300 X - band spectrometer. The system is equipped with a low temperature cavity allowing measurements to be made from room temperature down to 4K. For the FMR measurements performed on the melt spun ribbon samples the external field was varied in the ribbon plane over a range of 180°, while those on the discontinuous multilayers, the field was varied from the in-plane to out-of-plane directions.

3. Elements of ferromagnetic resonance theory

In general, when we consider the dynamic situation which prevails in an FMR type experiment we can apply the Landau - Lifshitz – Gilbert (LLG) equation of motion, which has the form:

$$\frac{1}{\gamma_i} \frac{\partial \underline{M}_i}{\partial t} = (\underline{M}_i \wedge \underline{H}_i^{eff}) - \frac{\alpha_i}{M_i} \left(\underline{M}_i \wedge \frac{\partial \underline{M}_i}{\partial t} \right), \quad (1)$$

where \underline{M}_i indicates the magnetisation of phase i , γ_i its magnetogyric ratio, α_i the Gilbert damping parameter and \underline{H}_i^{eff} the effective field to which it is subject at resonance. This effective field will contain the various contributions which make up the field felt by the magnetic spin system, such that:

$$\underline{H}^{eff} = \underline{H}_0 + \underline{h} + \underline{H}_K + \underline{H}_{ex} - \underline{H}_D, \quad (2)$$

where \underline{H}_0 is the static applied field at resonance, \underline{h} the microwave (driving) field, \underline{H}_K the anisotropy field, \underline{H}_{ex} the effective exchange field and \underline{H}_D the demagnetising field arising from sample shape effects. If we take a single phase system, the solution of the LLG equation yields the general resonance equation of the form:

$$\left(\frac{\omega}{\gamma} \right)^2 = \left(\frac{2A}{M} k^2 \right)^2 + \left\{ \frac{1}{M \sin^2 \vartheta} \frac{\partial^2 E}{\partial \phi^2} + \frac{1}{M} \frac{\partial^2 E}{\partial \vartheta^2} \right\} \left(\frac{2A}{M} k^2 \right) + \frac{1}{M^2 \sin^2 \vartheta} \left\{ \frac{\partial^2 E}{\partial \vartheta^2} \frac{\partial^2 E}{\partial \phi^2} - \left(\frac{\partial^2 E}{\partial \vartheta \partial \phi} \right)^2 \right\} \quad (3)$$

Here E represents the magnetic free energy of the system and will have contributions from the Zeeman, demagnetising and magnetocrystalline energies [3]. In equation (3) k represents the spin wave wavevectors and A the exchange stiffness constant. This equation is quadratic in the spin wave term. In the case of pure FMR, $k = 0$ and equation (3) reduces to the well known Smit – Beljers form.

To obtain a solution to equation (3) we need to take the partial derivatives of the magnetic free energy. The first derivatives can be set to zero to obtain the equilibrium conditions while the second derivatives are substituted into equation (3) to give the fully angular dependent resonance equation [3, 10].

4. Results and discussion

4.1. FeZrCuB amorphous / nanocrystalline ribbons

Amorphous and nanocrystalline materials are typically produced by the melt-spining technique, whereby amorphous ribbons are subject to partial devitrification by an appropriate thermal annealing treatment [11-13], and ultimately culminates in the production of a material which consists of randomly oriented ultrafine ferromagnetic nanocrystallites (~20Å) embedded in an Fe rich ferromagnetic matrix. The magnetic exchange coupling between these two phases suppresses local magnetocrystalline anisotropy and results in the extremely soft magnetic properties of this class of magnetic material [14]. In this section we shall discuss some results of FMR studies in the FeZrCuB system. In this alloy the devitrification process produces α -Fe nanograins in an Fe depleted but ferromagnetic amorphous matrix.

In Fig. 1 we display the variation of the resonance fields of the amorphous and nanocrystalline Fe phases as a function of the annealing temperature, T_{ann} . In the as-quenched state the alloy presents a single amorphous ferromagnetic phase with a single resonance peak. The phase separation of the Fe nanocrystallites is clearly observed after an annealing treatment of 350°C, with the appearance of a new resonance line at low fields, i.e. that due to the α -Fe phase. With further annealing at higher temperatures, we observe a gradual evolution of the two magnetic phases, whereby the Fe resonance gets stronger and shifts to lower fields, while that of the amorphous phase decreases in intensity and moves up in field, consonant with a reduction of magnetisation as the Fe content of this phase decreases.

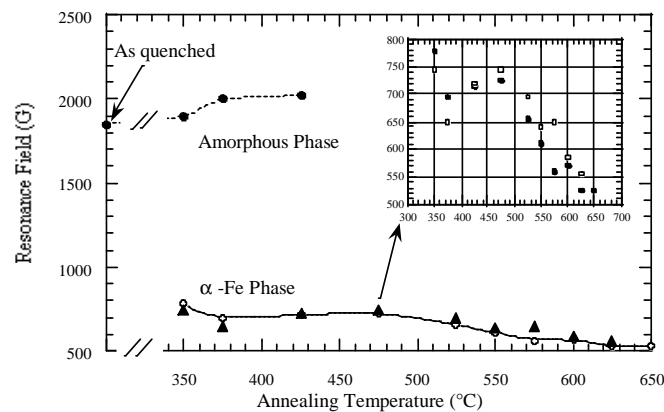


Fig 1. Resonance field position as a function of the annealing temperature for the $\text{Fe}_{87}\text{Zr}_6\text{Cu}_1\text{B}_6$ system for the α -Fe nanocrystalline phase and the remaining amorphous matrix. The inset shows an expanded view of the α -Fe phase resonance line.

Using a two phase approach to the problem we can evaluate the strength of the magnetic coupling between the amorphous and nanocrystalline magnetic phases and investigate its variation with annealing temperature as the two magnetic phases change in magnetic properties [10]. After annealing to over 475°C, the amorphous phase ceases to display a ferromagnetic resonance signal and the system effectively resembles a granular alloy. However, it has been shown that there is an Fe-rich interface region surrounding the Fe crystallites which plays an important role in the global magnetic properties of the samples [4]. This can most readily be displayed by evaluating the effective magnetisation of the Fe phase, see Fig. 2. The effective magnetisation is evaluated by fitting the variation of the resonance field as a function of the direction of the applied field [15].

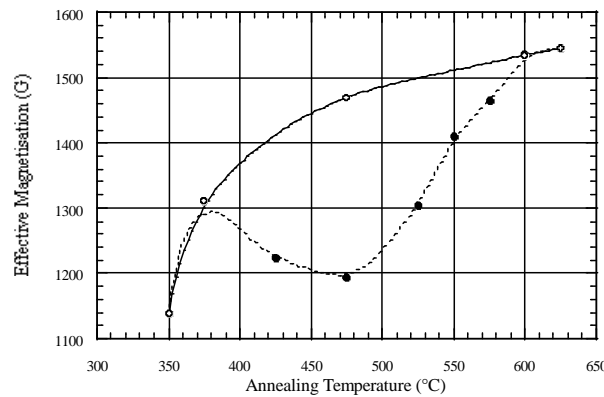


Fig. 2. Variation of the effective magnetisation for the Fe phase as a function of annealing temperature. The dashed line shows that experimental variation while the solid line indicates the variation expected for simple Fe grain growth.

The reduction of M_{eff} , instead of the expected monotonic increase for crystallite growth, is due to the strong coupling with the interphase region, which has a lower magnetisation than Fe. The interphase volume reaches a maximum where M_{eff} is a minimum and then reduces as this disordered

region gradually crystallises into the Fe grains and other phases. The effective magnetisation then gradually meets the expected increase and the ferromagnetic interphase region around the crystallites vanishes. Here the effective magnetisation is given by [4]:

$$M_{eff} = \frac{V_A M_A^2 + V_B M_B^2}{V_A M_A + V_B M_B} \quad (4)$$

where V represents the relative volume of the grains and the interphase regions, indicated by the A and B subscripts, respectively. Angular studies have shown that we can evaluate the magnetic constants, due to shape effects, and are given in ref. [15].

The linewidth also provides some useful indications of the magnetic state of the sample as a function of the annealing temperature, see Fig. 3. Any ferromagnetic sample will have an intrinsic linewidth, ΔH_0 , due to relaxation processes. The observed linewidth is very often much broader than this due to several broadening contributions. We can represent the measured linewidth in the following form:

$$\Delta H = \Delta H_0 + \Delta H_{cryst} + \Delta H_i + \Delta H_{vol} \quad (5)$$

The second term represents broadening due to variations in crystalline axes, the third term is that due to magnetic inhomogeneities in the sample and the last term is the broadening due to variations in grain size.

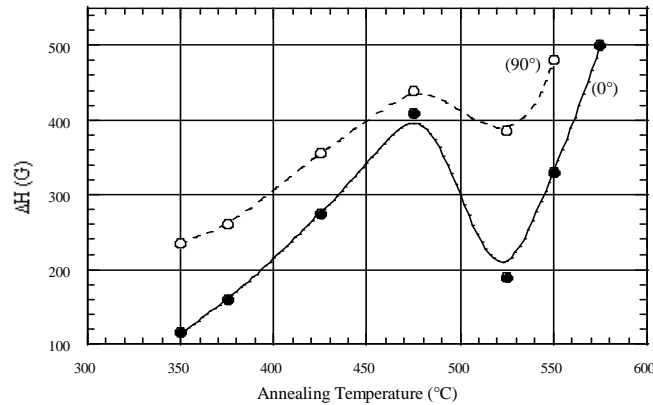


Fig. 3. Variation of the resonance linewidth for the Fe phase as a function of annealing temperature, (0° and 90° refer to the in-plane direction of the applied field along and across the ribbon direction, respectively).

In Fig. 3 we observe a substantial increase of the Fe resonance linewidth with a maximum at $T_{ann} = 475^\circ\text{C}$. This is mainly due to the presence of the interphase region formed in the proximity of the α -Fe nanocrystallites: As the interphase increases in size, its resonance overlaps with that of pure Fe phase. When the Fe-rich interphase region begins to crystallise into the pure Fe phase, its' resonance becomes weaker and the resulting spectra are narrower. This is evidenced by the sharp drop in ΔH above 500°C . With further annealing the Fe linewidth undergoes another increase due to increases in the second and fourth terms of equation (5), inhomogeneities may also play a rôle in the broadening. It is difficult to separate the various contributions to the broadening.

4.2. $\text{Fe}_x\text{Al}_{1-x}$ melt spun ribbons, $0.695 < x < 0.725$

The binary FeAl system provides a rich spectrum of physical properties with variation in composition and has attracted much interest over the years due to its mechanical and magnetic properties [16-18]. While at the Fe rich end of the phase diagram, the alloy is ferromagnetic, having an A2 disordered bcc crystallographic structure, with more than 30% Al the alloy becomes paramagnetic with DO_3 bcc ordering [17]. The ferromagnetic – paramagnetic (FM-PM) transition is more complex than the FeAl phase diagram would suggest and has been the subject of recent studies [5, 7] which indicate that the ferromagnetic breakdown is caused by a ferromagnetic clustering. That is, the sample is characterised by two regions, one of which consists of ferromagnetic clusters, while

the remaining regions is paramagnetic. Neutron reflectivity measurements have indicated a FM cluster size of the order of about 25\AA [19] for the $\text{Fe}_{70}\text{Al}_{30}$ sample and this sample has been shown to display superparamagnetic behaviour [7] due to the cluster like magnetic structure. To study the transition region (FM-PM) in further detail we have measured samples with $x = 0.725, 0.705, 0.70$ and 0.695 by ferromagnetic resonance as a function of sample temperature. The $\text{Fe}_{72.5}\text{Al}_{27.5}$ sample is mainly ferromagnetic in character and is used to distinguish those samples in the transition region while still expected to have paramagnetic regions. In Fig. 4 we show the temperature evolution of the resonance field as a function of temperature. Mössbauer spectroscopy and magnetic measurements on these samples have been reported elsewhere [5, 7] and are consistent with the FMR measurements. It has been conjectured that the size of the ferromagnetic clusters vary proportionally with sample temperature and for the $\text{Fe}_{70}\text{Al}_{30}$ sample there is a strong overlap in the cluster network [7]. Below $\sim 180\text{K}$ this overlap begins to recede and the clusters become disconnected resulting in a magnetic isolation below 50K where the sample becomes completely superparamagnetic.

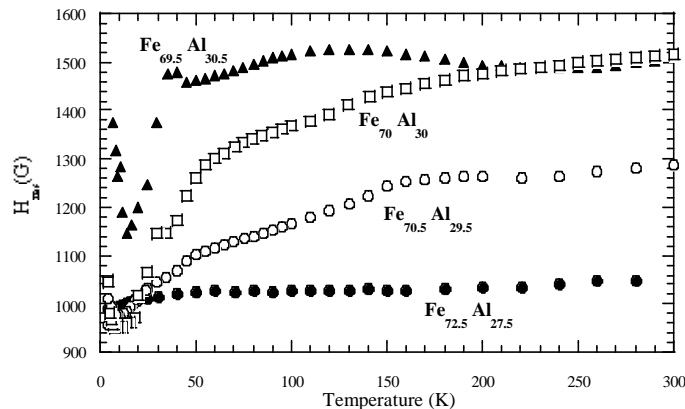


Fig. 4. Variation of the resonance field for the FeAl alloys as a function of temperature.

While the sample with 27.5% Al shows a rather weak variation of H_{res} with temperature, samples with Al concentrations at the FM-PM transition are extremely sensitive to temperature. The small decrease of H_{res} for the 27.5% Al sample down to $T \sim 40 - 50\text{K}$ is most probably almost entirely due to the variation of the magnetisation, since the sample is characterised by mainly ferromagnetic behaviour. This is not so for the samples at the FM-PM transition, where the samples show a cluster like magnetic structure. The variations of H_{res} are very large and we observe some significant changes in the slope, one at $\sim 150\text{K}$, which marks the onset of disconnection between the magnetic clusters as they begin to reduce in size and another at $\sim 50\text{K}$ which is related to the temperature at which the magnetic cluster become magnetically isolated. At lower temperatures a very marked minimum ($\sim 10\text{K}$) is observed in all samples. This maybe due to some surface effect at the boundaries between the FM and PM regions of the samples. In general we also note that the resonance field is inversely proportional to the Fe content as expected for samples with lower magnetisations.

Angular studies in these samples are not as conclusive as those for the amorphous and nanocrystalline materials of the previous section, where we are able to extract the material constants from a fitting of the angular variation of the resonance field. In this case we are dealing with a sample which is effectively a granular alloy and shape effects alone were not sufficient alone. The problem arises also from the fact that the magnetic character is effectively changing as a function of temperature, as observed in Fig. 4. Recent studies by small angle neutron scattering (SANS) provide clear indications that there is a change in cluster size and separation as a function of temperature [20]. In light of these data we need to assess how the various effects of intercluster interaction and size affect the overall properties of the sample and it is therefore not a simple task to retrieve the sample's magnetic constants at one particular temperature from the FMR data alone. One of the most important results from the SANS experiment shows the variation of the exchange correlation length as a function of temperature, where for the $\text{Fe}_{70}\text{Al}_{30}$ sample the effective cluster size reduces strongly below 150K . For temperatures below 50K the cluster size is of the order of 20\AA . A full

discussion of this data is beyond the scope of the present article and will be the subject of a future publication [20].

In Fig. 5 the resonance linewidth is shown as a function of the sample temperature. For the samples in the vicinity of the FM-PM transition composition there are some very large variations, while the sample which has a strong ferromagnetic nature (27.5% Al), the changes are relatively weak. The three samples in the region of the FM-PM transition display the same variations with temperature, where decreasing T from room temperature we observe a significant increase of the measured linewidth. A plateau region is evident where the linewidth reaches a maximum. This would imply that the samples reaches a state of maximum inhomogeneity, arising from the last two terms of equation (5). It should be clear that the variation in cluster size and the interaction between neighbouring magnetic particles will have a strong effect on the linewidth as well as the resonance field. From equation (5), we can deduce that the temperature variation of the linewidth should follow the form:

$$\Delta H(T) = \Delta H_i(T) + \Delta H_{vol}(T) \quad (6),$$

since we do not expect important variation of intrinsic and crystalline contributions as a function of temperature. At low temperatures, $T < 50$ K, the cluster size effectively stabilises and become magnetically isolated. Below 50K the linewidth reduces and we observe a minimum at around 10K, as also evident in the resonance field variation with temperature. Such a decrease in both the resonance field and linewidth could therefore be due to the reduction and disappearance of the interaction between magnetic particles. It is also worth noting that the linewidth increase for samples with lower Fe content in the small compositional range in the FM-PM transition region. This is probably related to the cluster size and the increased influence of the interface region at the FM cluster surface. It is very likely that the surface effects are dominant in the changes at low temperatures in the linewidth variation. A fuller analysis of the FMR data will be presented in a future publication [21].

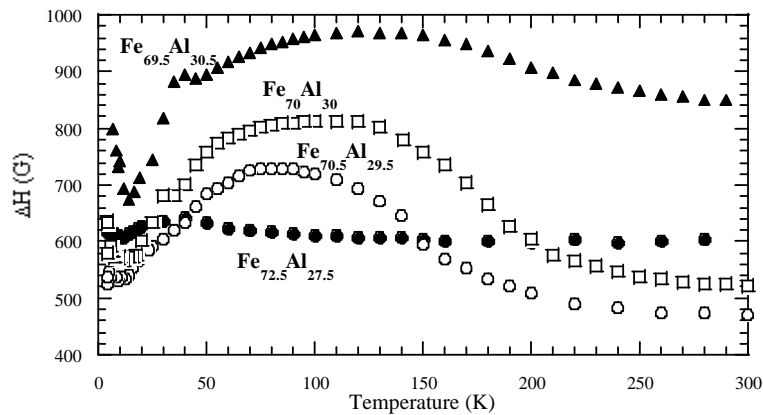


Fig. 5. Variation of the resonance linewidth for the FeAl alloys as a function of temperature.

4.3. Discontinuous multilayer system, $[\text{Al}_2\text{O}_3/\text{CoFe}(t)]_{10}\text{Al}_2\text{O}_3$

As mentioned previously, this system can be envisaged as a quasi 2D granular material in the t range studied. Since the intervening nonmagnetic matrix is insulating, we only expect interactions being due to a dipolar mechanism with RKKY type interactions being excluded. We can see that the strength of the dipolar interaction between the nanograins increases as we increase the effective equivalent thickness of the CoFe layer as expected, see Fig. 6. This is seen from the angular variation of the resonance field, in-plane to out-of-plane. Where we note that the larger the variation, that larger the dipolar interaction. This is due to the presence of the dipolar field from neighbouring islands and this will alter the internal magnetic field that is felt by the grains, and the field required to satisfy the resonance condition is therefore proportionally higher.

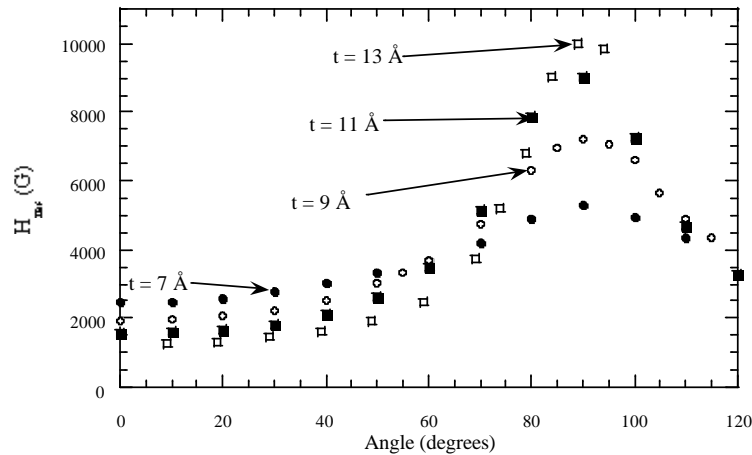


Fig. 6. Angular variation of the resonance field from in-plane (0°) to out-of-plane (90°).

In Fig. 7 we show the temperature dependence of the resonance field for the in-plane orientation of the applied external field. While the initial reduction of the resonance field, from room temperature, is to be expected, the dramatic enhancement of H_{res} below 90K is not. It will be immediately noticed that the size of this enhancement is inversely proportional to the effective thickness, or more significantly to the surface area to volume ratio. Such an observation would point to some grain surface effect, and most probably surface anisotropy, where we note that the influence of the surface and hence surface anisotropy will be expected to be proportionately greater for smaller islands since a larger proportion of its' atoms are in the region of the surface.

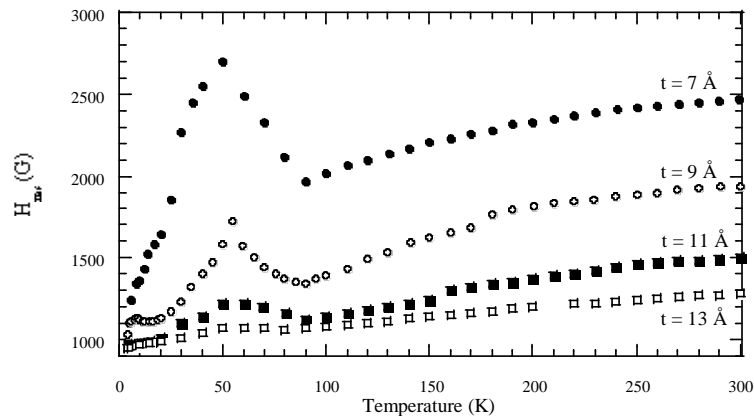


Fig. 7. Temperature dependence of the resonance field for the discontinuous multilayers $[\text{Al}_2\text{O}_3/\text{CoFe}(t)]_{10}\text{Al}_2\text{O}_3$ with $t = 7, 9, 11, 13 \text{ \AA}$.

At the lower end of the temperature range when the resonance field decreases, we observe a small shoulder. It is also curious to note that the resonance field tends to the same value for all the samples at around 4K. These preliminary results show some strong evidence for the importance of surface anisotropy in magnetic particulate systems. Theoretical studies have shown some of the complex static spin patterns that can be expected, from throttle to hedgehog structures, due to the effects of surface anisotropy [22]. The situation can therefore be expected to be equally complex in a dynamic situation. In the static condition, each spin orientation in the magnetic particle will be determined by the local internal field. In the dynamic case, as in an FMR experiment, we can expect that each spin environment will have its own particluar resonance condition, which is satisfied at slightly different applied external fields. In this case it can be expected that the external (surface) spins will resonate at very different values of applied field to those in the interior of the particle. This will produce the very broad resonances that are observed in these nanoparticulate systems [23].

5. Conclusion

We have shown that the ferromagnetic resonance technique is indeed very sensitive to changes in magnetic structure. This sensitivity is observed both through the direct measurement of the resonance field and from the linewidth of the resonance itself. Due to the nature of the samples it can be rather complex to extract all the material constants from just FMR measurements. In certain cases, as in the amorphous and nanocrystalline materials, angular studies can be effective in obtaining such information. In the cluster type materials, this can be more difficult and further information and measurements are necessary.

As we noted above, the very nature of nanoparticulate systems is likely to produce resonances which are very broad and extremely sensitive to external changes in environment (applied field strength and orientation and sample temperature). In fact, in the temperature dependent measurements on the FeAl and $[\text{Al}_2\text{O}_3/\text{CoFe}(\text{t})]_{10}\text{Al}_2\text{O}_3$ discontinuous multilayer system, we observe some very large variations of the resonance field and linewidth. It is very likely that for nanometric systems the surface effects are of vital importance in the overall properties manifested both in static and dynamic situations. The fact that there is strong evidence for the complex throttle and hedgehog like static spin structures in magnetic particles, we can expect an equally complex dynamic situation. In fact we suggest that we can no longer apply the classical FMR theory, and a solution of the resonance condition for each individual spin in the magnetic structure will be necessary since we are in a non-saturated state. That is due to the differences in the local internal magnetic field experienced by the different magnetic sites in the particle, different resonance conditions will be satisfied for different external fields. This means we should apply the LLG equation separately for each spin in turn, taking into account the various contributions to magnetic anisotropy and interactions and coupling with neighbouring spins and other magnetic particles in the vicinity.

Acknowledgements

Authors would like to thank CRUP of Portugal and the MCT of Spain for financial support in the form of a bilateral agreement N° E-31/03.

References

- [1] R. Skomski, *J. Phys.: Condens. Matter*, **15**, R841, (2003).
- [2] J. L. Martín, J. Nogués, K. Liu, J. L. Vincent, I. K. Schuller, *J. Magn. Magn. Mater.*, **256**, 449, (2003).
- [3] S. V. Vonsovskii, *Ferromagnetic Resonance*, Pergamon Press, Oxford, (1966).
- [4] D. S. Schmool, J. S. Garitaonandia, J. M. Barandiarán, *Phys. Rev. B* **58**, 12159, (1998).
- [5] D. S. Schmool, E. A. Araújo, M. M. Amado, M. Alegria Feio, D. Martín Rodríguez, J. S. Garitaonandia, F. Plazaola, *J. Magn. Magn. Mater.*, accepted for publication.
- [6] J. S. Garitaonandia, D. S. Schmool, J. M. Barandiarán, *Phys. Rev. B* **58**, 12147, (1998).
- [7] J. S. Garitaonandia, E. Apiñaniz, F. Plazaola, submitted to *Phys. Rev. B*.
- [8] G. N. Kakazei, Yu. G. Pogorelov, A. M. L. Lopes, J. B. Sousa, S. Cardoso, P. P. Freitas, M. M. Pereira de Azevedo, E. Snoeck, *J. Appl. Phys.*, **90**, 4044, (2001).
- [9] G. N. Kakazei, P. P. Freitas, S. Cardoso, A. M. L. Lopes, M. M. Pereira de Azevedo, Yu. G. Pogorelov, J. B. Sousa, *IEEE Trans. Magn.*, **35**, 2895, (1999).
- [10] D. S. Schmool, J. M. Barandiarán, *J. Phys.: Condens. Matter*, **10**, 10679, (1998).
- [11] Y. Yoshizawa, S. Oguma, J. Yamauchi, *J. Appl. Phys.*, **64**, 6044, (1988).
- [12] G. Herzer, *IEEE Trans. Magn.*, **26**, 1397, (1990).
- [13] K. Suzuki, A. Makino, A. Inoue, T. Matsumoto, *Mater. Trans. JIM*, **32**, 93, (1991).
- [14] I. Navarro, M. Ortuño, A. Hernando, *Phys. Rev. B* **53**, 11656, (1996).
- [15] D. S. Schmool, J. M. Barandiarán, *J. Magn. Magn. Mater.*, **191**, 211, (1999).
- [16] A. Taylor, R. M. Jones, *J. Phys. Chem. Solids*, **6**, 16, (1958).

- [17] G. Frommeyer, J. A. Jiménez, C. Derder, *Z. Metallkd.*, **90**, 930, (1999).
- [18] Y. Yang, I. Baker, P. Martin, *Phil. Mag. B*, **79**, 449, (1999).
- [19] K. Motoya, S. M. Shapiro, Y. Muraoka, *Phys. Rev. B* **28**, 6183, (1983).
- [20] J. J. del Val, J. S. Garitaonandia, F. Plazaola, D. Martín Rodríguez, D. S. Schmool, Unpublished.
- [21] D. S. Schmool, D. Martín Rodríguez, J. S. Garitaonandia, F. Plazaola, Unpublished.
- [22] H. Kachkachi, M. Dimian, *Phys. Rev. B* **66**, 174419, (2002).
- [23] D. S. Schmool, R. Rocha, G. N. Kakazei, J. A. M. Santos, J. B. Sousa, Unpublished.